Journal of Mathematics in Industry
a SpringerOpen Journal

RESEARCH Open Access

On simulations of spinning processes with a stationary one-dimensional upper convected Maxwell model

Maike Lorenz, Nicole Marheineke[1*] and Raimund Wegener[2]

*Correspondence:
marheineke@math.fau.de
[1]Department Mathematik, Friedrich-Alexander-Universität Nürnberg-Erlangen, Cauerstr. 11, Erlangen, 91058, Germany
Full list of author information is available at the end of the article

Abstract

This work deals with the behavior of viscoelastic jets under gravitational forces described by an asymptotic upper convected Maxwell (UCM) model, system of partial differential equations. Considering fiber spinning, we show that the one-dimensional model equations in general allow for the simulation of drawing processes with and without die swell effect. But, as the model is of hyperbolic type and the run of the characteristics crucially depend on the physical parameters, the existence regimes of the stationary solutions associated to certain boundary conditions turn out to be limited. We investigate the regimes for gravitational uniaxial and 2d spinning scenarios numerically.

Keywords: nonlinear viscoelasticity; UCM fluid; fiber spinning; die swell; boundary value problem; existence of solutions

1 Introduction

Fiber manufacturing is of special importance in communication, textile, automotive and building industry. Typical products are glass fibers, filters, insulating material, diapers or textile clothing. There are a variety of production processes, such a drawing with a take-up wheel, spunbond, meltblowing, rotational or electro-spinning, [1–5]. In general, a fluid (polymeric liquid or glass melt) is emerged from a orifice, pulled and stretched by outer forces to form a long thin fiber. The fiber jets can be considered as dynamic slender bodies. Topic of this work are viscoelastic jets. When spun, they might show a die swell effect, i.e. the fluid flow swells after exiting the nozzle and forms out a diameter that is significantly larger than the nozzle diameter. For small extrusion velocities the onion-shape rises directly at the nozzle, whereas for large velocities the swelling may happen away from the nozzle (delayed die swell), see [6, 7]. In industrial processes the forming of a die swell is undesirable since it changes the flow properties of the non-Newtonian fluid and consequently the quality of the resulting fabric. Hence, the understanding and prediction of this phenomenon is of special interest.

There exist a lot of viscoelastic models differing in the constitutive equation (e.g. Maxwell, Jeffrey, Oldroyed-B, Giesekus, Phan-Tien and Tanner models). We focus here on the (non-linear) upper convected Maxwell (UCM) model. It is form invariant under translation and rotation, and obeys the principle of material frame indifference (i.e. the observed phenomena are independent of the inertial frame in which they are observed).

Moreover, it is suitable for large deformation gradients. Additionally, and in contrast to more complex models such as the Giesekus or Phan-Thien and Tanner models, it is always evolutionary, i.e. stable with respect to short wave length perturbations. Limitations of the UCM model include the lack of multiple relaxation time scales as well as unbounded stress growth for extensional flow [8, 9]. In dimensionless form this single relaxation time occurs in the Weissenberg number We that is the product of a typical velocity gradient and a characteristic relaxation time.

Simulations of a Maxwell fluid as three-dimensional free boundary value problem include the die swell effect [10, 11], but fail for large Weissenberg numbers, see large We-limit in [12]. Because of the slender jet geometry, these simulations require a high refinement and are computationally very expensive. Hence, asymptotic models have been derived, see e.g. [13–15]. The aim of this paper is the investigation of the one-dimensional UCM model in [16] describing a dynamic curved jet by a time-dependent arc-length parameterized curve. We explore the applicability (solution regime) and the properties of the model, in particular whether it allows for a die swell.

As for the structure of this paper, we start with a brief introduction of the one-dimensional UCM model [16], followed by a classification in Section 2. The characteristic type of the partial differential system turns out to be determined by two classifying functions that limit the existence regime of stationary solutions, Section 3. In Sections 4 and 5 we investigate the applicability of the UCM model to stationary gravitational uniaxial and 2d spinning scenarios, respectively. We present numerical simulations of the jet behavior for different parameter ranges.

2 Asymptotic UCM model and its classification

The asymptotic upper convected Maxwell model of [16] in dimensionless form is given by

$$
\begin{aligned}
&\partial_t A + \partial_s(uA) = 0,\\
&\mathrm{Re}\big(\partial_t A\mathbf{v} + \partial_s(uA\mathbf{v})\big) = \partial_s(A\sigma\,\partial_s\boldsymbol{\gamma}) + A\mathbf{f},\\
&\mathrm{We}(\partial_t p + u\,\partial_s p + p\,\partial_s u) + p = -\partial_s u,\\
&\mathrm{We}\big(\partial_t\sigma + u\,\partial_s\sigma - (3p+2\sigma)\,\partial_s u\big) + \sigma = 3\,\partial_s u,\\
&\partial_t\boldsymbol{\gamma} + u\,\partial_s\boldsymbol{\gamma} = \mathbf{v}, \qquad \|\partial_s\boldsymbol{\gamma}\| = 1
\end{aligned}
\tag{1}
$$

for time $t \in \mathbb{R}^+$ and arc-length parameter $s \in (0, L(t))$ with jet length L. The balance, constitutive and coupling equations describe the dynamics and behavior of a viscoelastic jet with cross-section A, momentum-associated velocity $\mathbf{v}$, pressure p, stress component σ and jet curve $\boldsymbol{\gamma}$. The intrinsic (convective) speed u is the Lagrange multiplier to the arc-length constraint posed on $\boldsymbol{\gamma}$. The model is characterized by the dimensionless parameters: Reynolds Re and Weissenberg We numbers that denote the ratio of the inertial and viscous forces and the ratio of the relaxation and process time, respectively. By alternating the outer forces $\mathbf{f}$ and the boundary conditions, the system (1) is applicable to various scenarios, e.g. growing jet with free end, jet spinning with take-up wheel, inflow-outflow problem of fixed length. But the setting up of a well-posed problem is often difficult, as it is determined crucially by the closure conditions and the considered parameter regime as we will discuss.

In the terminology of Antman [17], there exist two classes of one-dimensional jet models: strings and rods. String models consist of balances for mass and linear momentum, whereas rod models cover additionally also angular momentum effects. Consequently, the system (1) is a viscoelastic string model prescribing the jet by help of the curve $\boldsymbol{\gamma}$. Thereby, it allows for the unrestricted motion and shape of $\boldsymbol{\gamma}$ and also covers the purely viscous case [18, 19] for We = 0. Moreover, it coincides with the uniaxial string model in [13, 20] for a straight UCM jet. In the uniaxial set-up jet curve and outer forces are similarly directed. For example, we have $\boldsymbol{\gamma} = s\mathbf{e_g}$ and $\mathbf{f} = \mathrm{Re}/\mathrm{Fr}^2\,\mathbf{e_g}$ for a straight jet under gravity with gravitational direction $\mathbf{e_g}$, $\|\mathbf{e_g}\| = 1$. The Froude number Fr denotes thereby the ratio of the inertial and gravitational forces. Consequently, the arc-length constraint vanishes; $\mathbf{v}$ becomes scalar-valued and equal to u:

$$\begin{aligned}
&\partial_t A + \partial_s(uA) = 0,\\
&\mathrm{Re}\big(\partial_t Au + \partial_s\big(Au^2\big)\big) = \partial_s(A\sigma) + Af,\\
&\mathrm{We}(\partial_t p + u\,\partial_s p + p\,\partial_s u) + p = -\partial_s u,\\
&\mathrm{We}\big(\partial_t\sigma + u\,\partial_s\sigma - (3p + 2\sigma)\,\partial_s u\big) + \sigma = 3\,\partial_s u.
\end{aligned} \tag{2}$$

For an uniaxial straight jet of fixed length in the absence of outer forces ($f = 0$) and Re = 0 the existence of unique solutions is proved under certain assumptions (regularity) in [15]. A general solution theory is not available so far, instead the solvability of the system turns out to be strongly dependent on the dimensionless parameters. Already, the three-dimensional upper-convected Maxwell equations lack solutions for high Weissenberg numbers [12]. For We = 0 the string model has also limitations [18]. Crucial for the evidence of viscous string solutions is the function q_1 [21, 22], in the more complex viscoelastic setting at hand we face additionally the relevance of the term q_2:

$$q_1 = u - \frac{1}{\mathrm{Re}}\frac{\sigma}{u}, \tag{3}$$

$$q_2 = 3 + \mathrm{We}(\sigma + 3p) - \mathrm{Re}\,\mathrm{We}\,u^2. \tag{4}$$

In this work we will refer to q_1 and q_2 as *classifying functions*.

To see the influence of q_1 and q_2 on the structure of the viscoelastic string model, we rewrite the system (1) as first order system in s and t. Therefore, we treat the curve's tangent $\boldsymbol{\tau} = \partial_s\boldsymbol{\gamma}$ as additional variable that fulfils $\partial_t\boldsymbol{\tau} = \partial_s\partial_t\boldsymbol{\gamma} = \partial_s(\mathbf{v} - u\boldsymbol{\tau})$ according to the coupling condition (for the velocities). Then we obtain the partial differential algebraic system

$$\begin{aligned}
&\mathbf{M}\cdot\partial_t\boldsymbol{\phi} + \mathbf{h}(\boldsymbol{\phi}, \partial_s\boldsymbol{\phi}) = \mathbf{0},\\
&\boldsymbol{\phi} = (A, \mathbf{v}, p, \sigma, \boldsymbol{\gamma}, \boldsymbol{\tau}, u), \qquad \mathbf{M} = \mathrm{diag}(1_{12}, 0), \qquad \mathbf{h}(\boldsymbol{\phi}, \boldsymbol{\psi}) = \mathbf{C}(\boldsymbol{\phi})\cdot\boldsymbol{\psi} + \mathbf{l}(\boldsymbol{\phi}) + \mathbf{g},
\end{aligned} \tag{5}$$

where $\mathbf{M} \in \mathbb{R}^{13\times 13}$ is a degenerated unit matrix with a zero entry in the last diagonal element. The classification of the system (5) is determined by the spectrum of matrix-valued function $\mathbf{C}$, we find the thirteen eigenvalues: $\lambda_1 = 0$ (multiplicity 4), $\lambda_2 = u > 0$ (multiplicity 3) and $\lambda_{3,4} = u \pm \sqrt{w}$ (multiplicity 3 each) with $w = u - q_1 u$. Hence, depending on the sign of w the system (5) changes its character. It is hyperbolic if $w > 0$ and mixed elliptic-

hyperbolic if $w < 0$. The case $w = 0$ yields an eigenvalue $\lambda = u$ of multiplicity 9, but with an eigenspace of dimension 5, involving a parabolic deficiency. Investigating the hyperbolic case - that is surely the most relevant one for the application - more deeply, $q_1 = 0$ separates two regimes with respect to the run of the characteristics, we have

$$\lambda_3 > 0, \qquad \lambda_4 < 0 \quad \text{for } q_1 > 0,$$
$$\lambda_{3,4} > 0 \quad \text{for } q_1 < 0.$$

An analogous classification and hyperbolic specification holds for the reduced uniaxial system (2), here $q_2 = 0$ separates the characteristic hyperbolic regimes. The system becomes

$$\begin{aligned} &\partial_t \boldsymbol{\varphi} + \mathbf{h}_{\text{uni}}(\boldsymbol{\varphi}, \partial_s \boldsymbol{\varphi}) = \mathbf{0}, \\ &\boldsymbol{\varphi} = (A, u, p, \sigma), \qquad \mathbf{h}_{\text{uni}}(\boldsymbol{\varphi}, \boldsymbol{\psi}) = \mathbf{C}_{\text{uni}}(\boldsymbol{\varphi}) \cdot \boldsymbol{\psi} + \mathbf{l}_{\text{uni}}(\boldsymbol{\varphi}) + \mathbf{g}_{\text{uni}} \end{aligned} \tag{6}$$

with four unknowns. The spectrum of $\mathbf{C}_{\text{uni}}$ consists of the eigenvalues $\lambda_{1,2} = u > 0$ and $\lambda_{3,4} = u \pm \sqrt{w}$ with $w = u^2 + q_2/(\text{Re We})$. Hence, the uniaxial system is hyperbolic if $w > 0$, mixed elliptic-hyperbolic if $w < 0$ and shows a parabolic deficiency for $w = 0$ (then $\lambda = u$ has multiplicity 4 with an eigenspace of dimension 2). The hyperbolic case is subdivided into two regimes by $q_2 = 0$,

$$\lambda_3 > 0, \qquad \lambda_4 < 0 \quad \text{for } q_2 > 0,$$
$$\lambda_{3,4} > 0 \quad \text{for } q_2 < 0.$$

The possible existence of different hyperbolic regimes depending on the physical parameters, such as Re, We and Fr, requires the careful consideration of the posed boundary conditions in view of the consistency and well-posedness of the problem (run of characteristics). This is also true in the viscous limit We = 0. In many spinning processes the long-time behavior of a jet becomes stationary. Moreover, the behavior close to the spinning nozzle is dominated by stationary effects. Hence, in the viscous case the issue of existing solutions was investigated comprehensively for a stationary jet [21–25]. The stationary viscoelastic string model is now topic in this work.

3 Transition to stationarity

Let us consider spinning processes which last long enough such that the jet up to a certain length L can be regarded as stationary. Let $L = 1$ be due to the applied dimensionless scaling. In order to obtain the stationary model equations we neglect the time dependencies in the system (5) - or the system (6), respectively. As the mass flux becomes constant, the cross-section A is related to the convective speed u and drops out of the equations, i.e. $A = 1/u > 0$. So, an arbitrary curved jet is described by

$$\begin{aligned} &\partial_s \boldsymbol{\gamma} = \boldsymbol{\tau}, \qquad \|\boldsymbol{\tau}\| = 1, \\ &q_1\, \partial_s \boldsymbol{\tau} = \frac{1}{u}\big(\mathbf{f} - (\mathbf{f} \cdot \boldsymbol{\tau})\boldsymbol{\tau}\big), \\ &q_2\, \partial_s u = \sigma - \text{We}\, u \mathbf{f} \cdot \boldsymbol{\tau}, \end{aligned} \tag{7}$$

$$\begin{aligned}
\mathrm{We}\,\partial_s p &= -\frac{1}{u}\big(\partial_s u(\mathrm{We}\,p+1)+p\big),\\
\partial_s \sigma &= \partial_s u\left(\mathrm{Re}\,u+\frac{\sigma}{u}\right)-\mathbf{f}\cdot\boldsymbol{\tau}
\end{aligned}$$

and a straight (uniaxial) jet by

$$\begin{aligned}
q_2\,\partial_s u &= \sigma - \mathrm{We}\,u\mathrm{B},\\
\mathrm{We}\,\partial_s p &= -\frac{1}{u}\big(\partial_s u(\mathrm{We}\,p+1)+p\big),\\
\partial_s \sigma &= \partial_s u\left(\mathrm{Re}\,u+\frac{\sigma}{u}\right)-\mathrm{B}
\end{aligned} \tag{8}$$

with $\mathrm{B} = \mathrm{Re}/\mathrm{Fr}^2$ in the gravitational set-up.

Depending on the choice of boundary conditions the classifying functions q_1 and q_2 may restrict the solvability of the system of ordinary differential equations (7); singularities can occur when $q_i(s^\star) = 0$, $s^\star \in (0,1)$, $i = 1,2$, cf. Equations (3) and (4). Studies [22, 25] of the stationary viscous string model (where $\mathrm{We} = 0$ and $q_2 = 3$) show that the loss of solutions arises as the underlying asymptotically derived model is singularly perturbed in q_1 for certain parameter regimes. In some scenarios and regimes the inconsistency of the degenerated equations and the boundary conditions can be eliminated by omitting the boundary conditions in favor of an other closing, yielding different string variants [21, 24]. These investigations made use of the monotonicity of q_1, i.e.

$$\partial_s q_1 = \frac{1}{\mathrm{Re}\,u}\mathbf{f}\cdot\boldsymbol{\tau} > 0$$

holds true because of the jet dynamics due to the acting forces. The monotonicity allowed the analytical determination of limiting hyperplanes and the numerical exploration of the different solution regimes. For $\mathrm{We} \neq 0$, the monotonicity of q_1 is kept. But the term q_2 leads to additional limitations which are even more difficult to predict since q_2 shows neither monotonicity nor other characteristic properties. In the uniaxial case (8) the term q_1 is not present such that we can exclusively focus on q_2.

In the following we study the applicability of the stationary asymptotic UCM model to the simulation of gravitational spinning processes. Thereby, we consider the uniaxial and the 2d set-ups.

Remark 1 For the numerical solution of the arising boundary value problems of ordinary differential equations we use a Runge-Kutta collocation method. The resulting systems of non-linear equations are solved via Newton's method.

4 Uniaxial spinning

The stationary models for the uniaxial spinning of viscoelastic and viscous jets show two difference. First, the viscoelastic solution regime may be limited by the root of q_2 depending on the chosen boundary conditions, whereas the viscous model ($\mathrm{We} = 0$, $q_2 = 3$) has solutions for all $(\mathrm{Re}, \mathrm{Fr})$. Second, the viscoelastic model admits solutions with a minimum in the velocity u for $s \in (0,1)$. For the viscous model it can be easily shown that any extremum of u in $(0,1)$ is a maximum. According to the stationary relation $A = 1/u$ for the

Figure 1 Sketch of a spinning process with die swell.

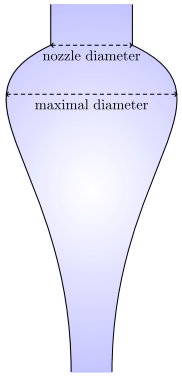

cross-sections we investigate whether this fact enables us to reproduce a die swell which is observed in experiments with viscoelastic fluids under gravity. The die swell is an effect where a fluid extruded from a capillary forms out a jet with a diameter that is significantly larger than the nozzle diameter [6] (see [7] for photos and Figure 1 for a sketch).

4.1 Drawing processes and die swell

In this section the question is addressed whether the uniaxial model allows for simulations of a die swell. To simplify the investigations we restate Equations (8) in terms of $b = \sigma - \mathrm{We}\,\mathrm{B}u$ and $a = q_2$

$$\begin{aligned}
\partial_s u &= \frac{b}{a},\\
\partial_s b &= \frac{b}{a}\left(\frac{b + \mathrm{Re}\,u^2}{u}\right) - \mathrm{B},\\
\partial_s a &= 2\frac{b}{a}\,\mathrm{We}\left(\mathrm{We}\,\mathrm{B} + \frac{b}{u} - \mathrm{Re}\,u\right) - \mathrm{Re}\,u + \frac{1}{\mathrm{We}\,u}(3-a).
\end{aligned} \tag{9}$$

The system is supplemented by three boundary conditions that we specify later on.

Definition 1 Let (u, b, a) be a continuously differentiable solution of the system (9) for arbitrary but fixed boundary conditions. We call $s^* \in (0,1)$ a point where a die swell occurs if $\partial_s u(s^*) = 0$ and $u(s^*)$ is a local minimum.

Among all possible solutions we are only interested in drawing processes as defined below which we consider to be the physically relevant solutions in this scenario.

Definition 2 (Drawing process) We call the solution of the system (9) a *drawing process*

- *without die swell* if $\partial_s u(s) > 0$ for all $s \in [0,1)$,
- *with die swell* if there exists exactly one $s^* \in (0,1)$ with $\partial_s u(s^*) = 0$, $\partial_s u(s) < 0$ for all $0 \le s < s^*$ and $\partial_s u(s) > 0$ for all $s^* < s \le 1$.

With the following lemmata we can exclude the occurrence of a die swell for the boundary condition $b(1) = 0$ that corresponds to a *constant velocity end* $\partial_s u(1) = 0$ (e.g. via a take-up wheel).

Lemma 1 *Let* (Re, We, Fr) *be given with* $\mathrm{B} \neq 0$ *and suppose that* (u, b, a) *is a continuously differentiable solution of the system* (9) *for arbitrary but fixed boundary conditions. Suppose that* $a \neq 0$ *for all* $s \in [0,1]$. *Then* b *can have at most one root on* $[0,1]$.

Proof For any root s^* in b we find that $\partial_s b(s^*) = -\mathrm{B}$. By continuity of b only one root can occur. □

Lemma 2 *Let* (Re, We, Fr) *and some* $D \in \mathbb{R} \setminus \{0\}$ *be given such that* $a(0) = D$ *or* $a(1) = D$. *Suppose that a continuously differentiable solution of the system* (9) *exists with* $u(0) = 1$, $b(1) = 0$ *and* $a \neq 0$ *for all* $s \in [0,1]$. *Then this cannot be a drawing process with die swell. Furthermore, this is only a drawing process if* $D > 0$.

Proof For a drawing process with die swell a root of $\partial_s u$ is required on $(0,1)$. This corresponds to a root in b at some $s^* \in (0,1)$. Due to the boundary condition and Lemma 1 this is not possible.

If $D < 0$, also $a < 0$ holds for all $s \in [0,1]$ and hence $b(1) = 0$ enforces a minimum in u such that the velocity is monotonically decreasing on $[0,1]$ which is not a drawing process. □

Similarly, we can derive necessary conditions for a drawing process with die swell, considering the boundary condition $b(1) = -\mathrm{We}\,\mathrm{B}u(1)$ that corresponds to a *stress-free end* $\sigma(1) = 0$.

Lemma 3 *Let* (Re, We, Fr) *and some* $D \in \mathbb{R} \setminus \{0\}$ *be given such that* $a(0) = D$ *or* $a(1) = D$. *Suppose that a continuously differentiable solution of the system* (9) *exists with* $u(0) = 1$, $b(1) = -\mathrm{We}\,\mathrm{B}u(1)$ *and* $a \neq 0$ *for all* $s \in [0,1]$. *Then this can be a drawing process with die swell. Furthermore, this is only a drawing process if* $D < 0$.

Proof Since the sign of D determines the sign of a we distinguish two cases:

$a > 0$: This is no drawing process because either u decreases monotonically (no root in b) or u first increases, then decreases and hence has a maximum (root in b).

$a < 0$: If b does not have a root, u increases strictly which implies a drawing process. If b has a root, it is a drawing process with die swell. □

With regard to our investigations and the time-dependent classification in Section 2, uniaxial drawing processes (DP) admit different sets of reasonable boundary conditions. First of all, the inflow velocity at the nozzle is prescribed by $u(0) = 1$ due to the applied dimensionless scaling. Then, we can distinguish between four categories.

Uniaxial DP Categories.

(A) $b(1) \geq 0 \wedge a(0) > 0$: *no die swell,*

(B) $b(0) < 0 \wedge a(0) < 0$: *no die swell,*

(C) $b(0) > 0 \wedge a(1) > 0$: *DP without die swell if and only if* $b(1) > 0$,

(D) $b(0) > 0 \wedge a(0) < 0$: *DP with die swell if and only if* $b(1) < 0$.

In Category (A) the practically relevant drawing processes with constant velocity end (e.g. driven by a take-up wheel) are contained. Drawing processes with die swell are described by Category (D) if and only if $b(1) < 0$. This implies a stress-free end.

4.2 Existence regime and jet dynamics

For the application, drawing processes of Categories (A) and (D) are of main interest. Therefore, we restrict here to the investigation of their solutions regimes. For Categories (B) and (C) see [26].

Category (*A*)

The parameter regime (Re, We, Fr) where solutions exist essentially depend on the run of the non-monotone function a (or respectively q_2). A root that characterizes a change-of-type of the corresponding time-dependent equations limits the regime. Although the classifying function is not monotone a systematic determination of the existence regime in the high-dimensional parameter space is possible because $a(1) \to 0$ for increasing Re. This substantiates our approach that follows the ideas of [22]. The aim is to find those parameters (Re, We, Fr) for which a solution of the boundary value problem of Category (A) exists with $a(1) = 0$. For the numerical treatment we impose the additional condition $a(1) = \delta$, $0 < \delta \ll 1$ in favor of We.

In Figure 2 the existence regime for $b(1) = 0$, $a(0) = 1$ and Fr = 2 is sketched using $\delta = 0.1$. The blue lines visualize the limiting curves found for varying Re, the green circles mark the parameters $(\mathrm{Re}, \mathrm{We}) \in [10^{-2}, 10^{2}] \times [10^{-7}, 6.2]$ for which numerical solutions exists. The area enclosed by both limiting curves does not allow for solutions. To capture all regions of the limiting curve we have to consider either We or Re as variable (depending on the gradient) and combine both results. With a combined search we can additionally vary Fr and obtain the corresponding limiting surface shown in Figure 3. In consistence with Figure 2 no solutions can be found for (Re, We, Fr) inside the volume enclosed by the limiting surface. Close to the viscous case ($\mathrm{We} \ll 1$) no limitations occur. For moderate values of We only small Reynolds numbers imply solutions, whereas larger Re require We to lie above the upper part of the limiting surface. This part grows more than linearly in We for increasing Froude numbers. Increasing $D \gg 1$ in $a(0) = D$ leads to comparably shaped limiting surfaces with a less restrictive regime of existence.

Solutions to this case are plotted in Figure 4, for $(\mathrm{We}, \mathrm{Fr}) = (1, 2)$ and varying Re.

Category (*D*)

For Category (D) we deal with initial value problems, whose classification of solutions is made by the sign of $b(1)$. The hyperplanes separating the drawing processes from the physically irrelevant solutions can be determined in the same spirit as above. For given Fr and Re find We such that a solution of the boundary value problem of Category (D) with $b(1) = 0$ exists. Certainly, also the roles of We and Re can be interchanged, then the condition $a(1) = -\delta$, $\delta \to 0$ need to be imposed instead.

Figure 5 shows the curves separating the die swell solutions (green circle) from the other solutions (red circle) for $b(0) = 1$, $a(0) = -1$ and Fr = 2. Be aware that the red curve does not represent the border of the existence regime. For $\mathrm{We} \to 0$ the solutions converge to the viscous solutions without die swell. The lack of circles comes from the incompatibility of the boundary condition $a(0) = -1$ and the viscous limit $a = q_2 = 3$ that causes boundary layers and finally the break-down of the numerics.

Two die swell solutions are visualized in Figure 6 for varying Reynolds and Weissenberg numbers. For increasing Re the point of the die swell moves closer to the nozzle $s = 0$. This is also observed for large Re, $\mathrm{Re} \sim \mathcal{O}(10^2)$. Increasing We has the opposite effect on the die swell point, it moves to $s = 1$. In both cases the minimal value of u grows larger.

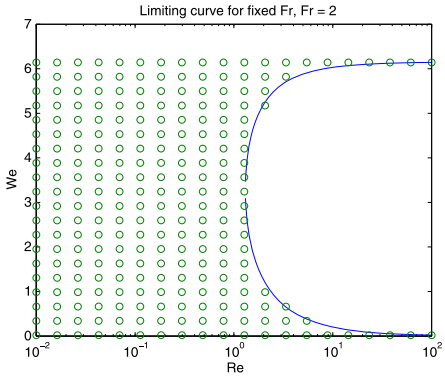

Figure 2 Existence regime for the uniaxial model, Category (A): limiting curve for $b(1) = 0$, $a(0) = 1$ and Fr = 2.

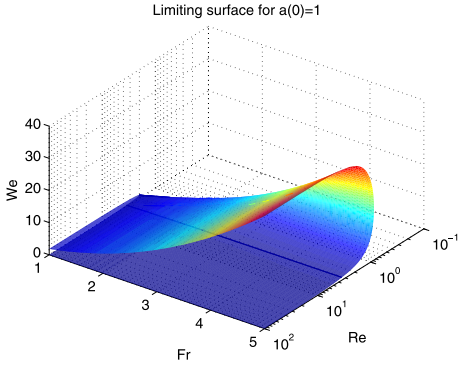

Figure 3 Existence regime for the uniaxial model, Category (A): limiting surface in correspondence to Figure 2.

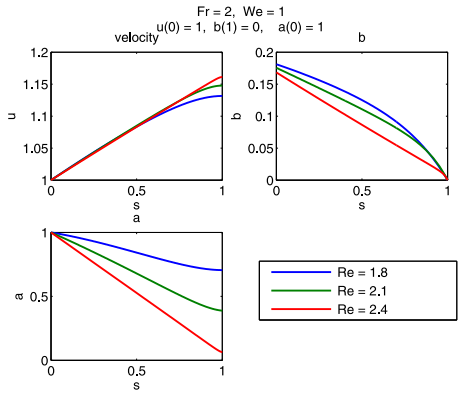

Figure 4 Jet behavior for the uniaxial model, Category (A): (We, Fr) = (1, 2) and varying Re.

5 Gravitational 2d spinning

In the gravitational 2d spinning set-up the fluid is extruded from the nozzle perpendicularly to the gravitational direction. In the absence of further outer forces the jet moves in a plane (e.g. $\mathbf{e_1}$-$\mathbf{e_2}$-plane) and its tangent $\boldsymbol{\tau}$ can be described by a single angle α. Without loss of generality we consider $\mathbf{f} = -\mathrm{B}\mathbf{e_2}$ and $\boldsymbol{\tau}(\alpha) = \cos\alpha\,\mathbf{e_1} + \sin\alpha\,\mathbf{e_2}$ with $\alpha(0) = 0$ in Equations (7). At the nozzle $s = 0$, the jet position and velocity are prescribed, i.e. $\boldsymbol{\gamma}(0) = \boldsymbol{\gamma_0}$ and $u(0) = 1$. Moreover, we impose $\sigma(1) + \mathrm{We}\,\mathrm{B}u(1)\sin\alpha(1) = 0$ for a end with constant velocity ($\partial_s u(1) = 0$), similarly as in [22] for the viscous jet. The last boundary condition we choose is $q_2(0) = D$, $D \neq 0$.

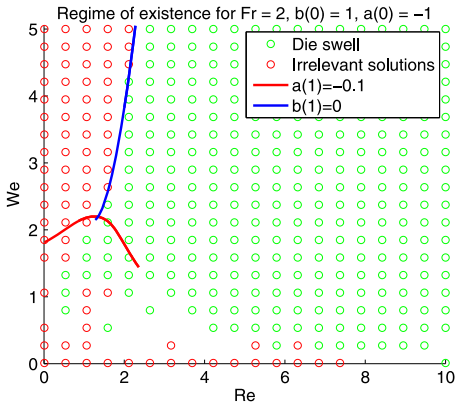

Figure 5 Die swell regime for the uniaxial model, Category (D): separating curves for $b(0) = 1$, $a(0) = -1$ and Fr = 2.

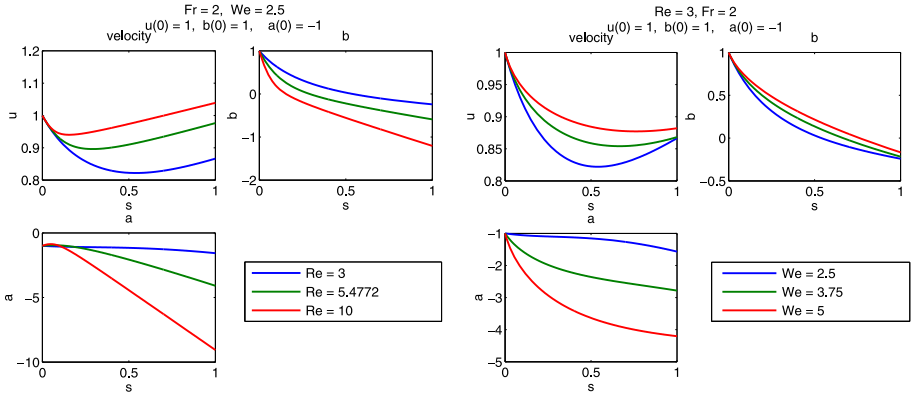

Figure 6 Die swell solution for the uniaxial model, Category (D): reference (Re, We, Fr) = (3, 2.5, 2) (blue curve). Left: variations in Re. Right: variations in We.

5.1 Existence regime

The gravitational 2d UCM model is similar to the gravitational 2d viscous model [22] with respect to q_1 (monotonically increasing) and similar to the uniaxial UCM model of Category (A) with respect to q_2 ($q_2(1) \to 0$). Hence the solution regime can be systematically investigated by imposing these two additional conditions $q_1(0) = 0$ and $q_2(1) = 0$ instead of two dimensional parameters. Numerically, we use $q_1(0) = q_2(1) = \delta$, $\delta \ll 1$ for the search, and apply a continuation-collocation strategy to keep track of grid points and function evaluations used. This procedure that was developed for the viscous case is faster and more robust than direct calculations of the next solution (see [22] for details).

Figure 7 shows the limiting surfaces with respect to q_1 and q_2 as well as their intersection in the parameter space (Re, We, Fr) for the case $D = 1$, $\delta = 0.1$ (compare with the results for the uniaxial UCM model, Category (A) in Figure 3).

5.2 Influence of parameters on jet behavior

The jet behavior (in terms of curve $\boldsymbol{\gamma}$, angle α, velocity u, pressure p and stress component σ) is influenced by the parameters Re, We and Fr. In the following, we consider a jet with $D = 1$, other boundary values $D > 0$ yield similar results. We have a drawing process with monotonically increasing velocity, no die swell forms out in agreement with the uniaxial investigations for Category (A).

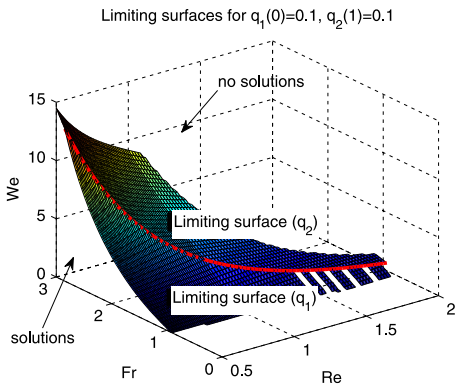

Figure 7 Existence regime for the gravitational 2d model: limiting surface for $q_2(0) = D = 1$.

Small Re imply a almost constant velocity. For increasing Re, the maximal velocity $u(1)$ grows larger. Also the stress profile rises, but its maximum is attained inside the interval $[0,1]$. The pressure tends to zero. As the Froude number is inversely proportional to gravity, the jet is more curved and accelerated for smaller Fr, implying higher velocity and stress. The effect is much more significant than for increasing Re. In contrast to the influence of the Reynolds number, the pressure attains lower values for lower Fr. The influence of We is comparable to the one of Re. For We $\to 0$ we observe the rising of a boundary layer in the pressure as $q_2(0) = D = 1$ is chosen instead of the viscous limit $q_2 = 3$. For the remaining variables the viscous solution and the UCM solution for We = 0.1 coincide well.

In Figure 8 the jet behavior around the reference solution associated to the parameter tupel $(\mathrm{Re}, \mathrm{We}, \mathrm{Fr}) = (1,1,2)$ (red curve) is visualized for varying Re, Fr and We, respectively. The parameter variations are thereby chosen with respect to the existence regime (Figure 7).

6 Conclusion and outlook

The one-dimensional upper convected Maxwell model [16] allows for the simulation of viscoelastic fiber spinning, in particular die swell effects can be reproduced. The stationary model for an uniaxial straight jet driven by gravity admits four different sets of boundary conditions: the occurrence of a die swell is analytically excluded for a constant velocity end, whereas it may arise for a stress free end. It remains an open question whether respective boundary conditions for a die swell can be motivated physically or whether further effects need to be considered in order to achieve numerical predictions that are comparable with experimental data.

The stationary asymptotic UCM model is a string model whose applicability turns out to be restricted to certain parameter ranges because of occurring singularities (singularly perturbed model). In contrast to the viscous case, this holds already true for the uniaxial UCM string. For other spinning set-ups the investigation of the solution regime requires the determination of the roots of - not only one, but - two classifying functions in a high-dimensional parameter space. A respective numerical search strategy is proposed and applied to the gravitational uniaxial and 2d spinning scenarios in this work. Its extension to industrial spinning processes is difficult and not productive when aiming for the simulation of the whole parameter regime. Instead of this, alternative asymptotic models that overcome the limitation should be asked for.

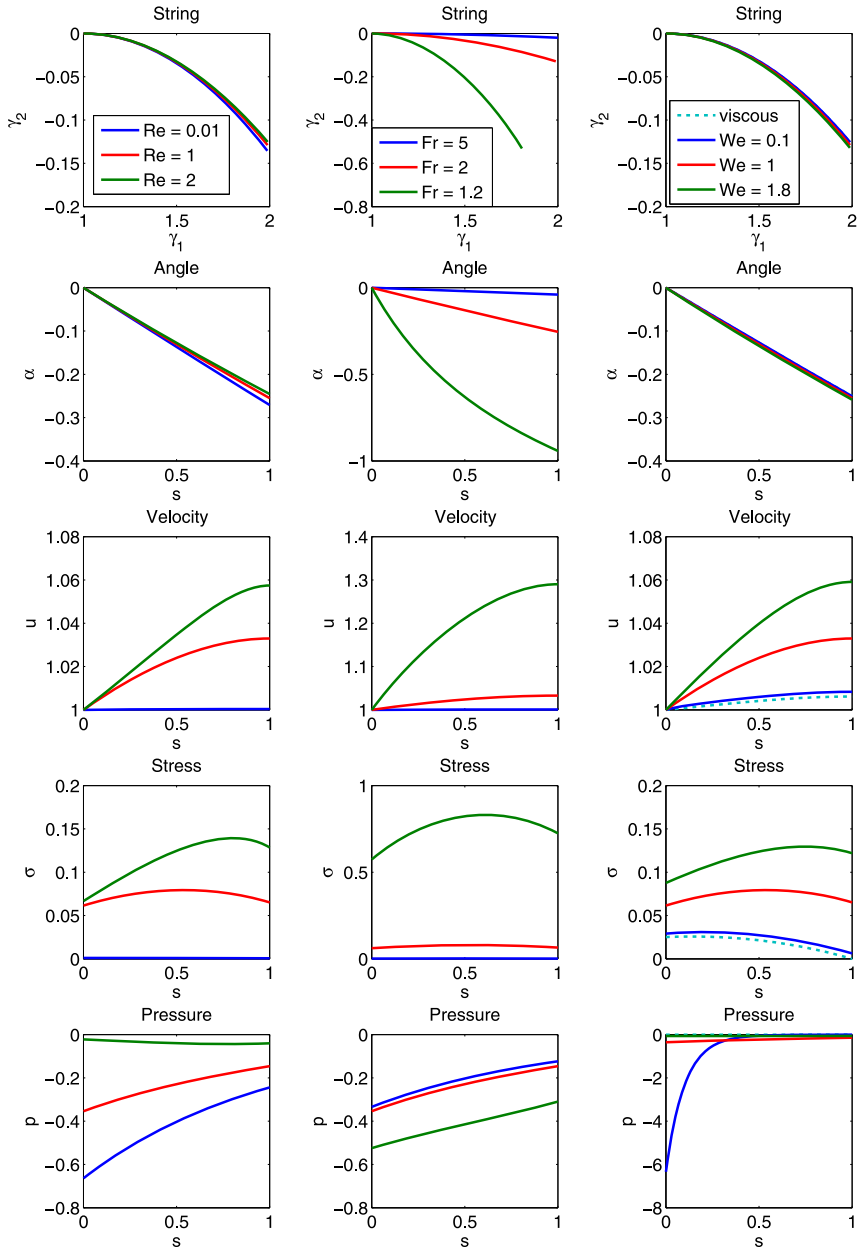

Figure 8 Jet behavior for the gravitational 2d model: reference (Re, We, Fr) = (1, 1, 2) (red curve). From left to right: variations in Re, variations in Fr, variations in We.

Competing interests
The authors declare that they have no competing interests.

Authors' contributions
The initial ideas were proposed by RW. Their elaboration (theoretical results and numerical simulations) was done by ML supported by RW and NM. NM wrote and approved the final manuscript.

Author details
[1]Department Mathematik, Friedrich-Alexander-Universität Nürnberg-Erlangen, Cauerstr. 11, Erlangen, 91058, Germany.
[2]Fraunhofer Institut für Techno- und Wirtschaftsmathematik, Fraunhofer Platz 1, Kaiserslautern, 67663, Germany.

Acknowledgements
This work has been supported by the Center for Mathematical and Computational Modeling $(\mathrm{CM})^2$, Kaiserslautern (Rhineland-Palatinate research initiative).

Received: 13 April 2013 Accepted: 7 March 2014 Published: 03 Jun 2014

References

1. Pearson JRA: *Mechanics of Polymer Processing*. Amsterdam: Elsevier; 1985.
2. Pinchuk LS, Goldade VA, Makarevich AV, Kestelman VN: *Melt Blowing: Equipment, Technology and Polymer Fibrous Materials*. *Springer Series in Materials Processing*. Berlin: Springer; 2002.
3. Ziabicki A, Kawai H: *High Speed Melt Spinning*. New York: Wiley; 1985.
4. Yarin AL: *Free Liquid Jets and Films: Hydrodynamics and Rheology*. New York: Longman; 1993.
5. Hohmann MM, Shin M, Rutledge G, Brenner MP: **Electrospinning and electrically forced jets. I. Stability theory**. *Phys. Fluids* 2001, **13**:2201-2220.
6. Bird RB, Armstrong RC, Hassager O: *Dynamics of Polymeric Liquids*. New York: Wiley; 1987.
7. Joseph DD: *Fluid Dynamics of Viscoelastic Liquids*. New York: Springer; 1990.
8. Larson RG: **Instabilities in viscoelastic flows**. *Rheol. Acta* 1992, **31**:213-263.
9. Joseph DD: **Hyperbolic phenomena in the flow viscoelastic liquids**. In *Trends in Applications of Pure Mathematics to Mechanics*. Edited by Kröner E and Kirchgässner K. *Lecture Notes in Physics*. Volume 249. Berlin: Springer; 1986:434-456.
10. Crochet MJ, Keunings R: **Die swell of a Maxwell-fluid: numerical prediction**. *J. Non-Newton. Fluid Mech.* 1980, **7**:199-212.
11. Crochet MJ, Keunings R: **On numerical die swell calculation**. *J. Non-Newton. Fluid Mech.* 1982, **10**:85-94.
12. Renardy M: **On the high Weissenberg number limit of the upper convected Maxwell fluids**. *J. Non-Newton. Fluid Mech.* 2010, **165**:70-74.
13. Schultz WW, Davis SH: **Slender viscoelastic fiber flow**. *J. Rheol.* 1987, **31**(8):733-750.
14. Forest MG, Wang Q: **Dynamics of slender viscoelastic free jets**. *SIAM J. Appl. Math.* 1994, **54**(4):996-1032.
15. Hagen TC: **On viscoelastic fluids in elongation**. *Adv. Math. Res.* 2002, **1**:187-205.
16. Lorenz M, Marheineke N, Wegener R: **On an asymptotic upper convected Maxwell model for a viscoelastic jet**. *Proc. Appl. Math. Mech.* 2012, **12**:601-602.
17. Antman SS: *Nonlinear Problems of Elasticity*. New York: Springer; 2006.
18. Panda S, Marheineke N, Wegener R: **Systematic derivation of an asymptotic model for the dynamics of curved viscous fibers**. *Math. Methods Appl. Sci.* 2008, **31**:1153-1173.
19. Marheineke N, Wegener R: **Asymptotic model for the dynamics of curved viscous fibers with surface tension**. *J. Fluid Mech.* 2009, **622**:345-369.
20. Schultz WW, Davis SH: **One-dimensional liquid fibres**. *J. Rheol.* 1982, **26**:331-345.
21. Hlod A, Aarts ACT, van de Ven AAF, Peletier MA: **Three flow regimes of viscous jet falling onto a moving surface**. *IMA J. Appl. Math.* 2012, **77**(2):196-219.
22. Arne W, Marheineke N, Wegener R: **Asymptotic transition of Cosserat rod to string models for curved viscous inertial jets**. *Math. Models Methods Appl. Sci.* 2011, **21**(10):1987-2018.
23. Götz T, Klar A, Unterreiter A, Wegener R: **Numerical evidence for the non-existence of solutions to the equations describing rotational fiber spinning**. *Math. Models Methods Appl. Sci.* 2008, **18**(10):1829-1844.
24. Hlod A, Aarts ACT, van de Ven AAF, Peletier MA: **Mathematical model of falling of a viscous jet onto a moving surface**. *Eur. J. Appl. Math.* 2007, **18**:659-677.
25. Arne W, Marheineke N, Meister A, Wegener R: **Numerical analysis of Cosserat rod and string models for viscous jets in rotational spinning processes**. *Math. Models Methods Appl. Sci.* 2010, **20**(10):1941-1965.
26. Lorenz M: **On a viscoelastic fibre model - asymptotics and numerics**. *PhD thesis*. Technische Universität Kaiserslautern; 2013.

10.1186/2190-5983-4-2
Cite this article as: Lorenz et al.: On simulations of spinning processes with a stationary one-dimensional upper convected Maxwell model. *Journal of Mathematics in Industry* 2014, 4:2